International Institute of Welding

JAPANESE DELEGATION

Phone : + 81 3 3257 1644

Fax : + 81 3 3255 5196 **Email : itoua@jwes.or.jp** **WEB Site : http://www.jwes.or.jp/**

I-1177-10

Study of Heat Transfer during Piercing Process of Oxy-fuel Cutting

Naoki Osawa, Junji Sawamura, Naoya Okamoto (Osaka University, Osaka, Japan)
Yuichi Ikegami (Air Water Inc., Osaka, Japan)

A generic algorithms (GA)-based identification technique for the heat transfer parameters, the gas temperature adjacent to the plate, T_G, and the local heat transfer coefficient, α, of the preheating gas flame of Oxy-fuel cutting is proposed. The validity of the proposed technique and the accuracy of the identified parameters are examined by comparing the measured and calculated plate back face temperatures during spot heating tests. Aqua gas and LPG are used as preheating gas in these tests. The minimum piercing time is estimated by calculating the time until the plate heating face temperature reaches the kindling temperature. The validity of the proposed piercing performance estimation method is examined by comparing the estimated and measured minimum piercing times for Aqua gas and LPG. As results, the followings are found.

1) The plate temperatures during spot heating tests calculated by using the identified T_G and α agree well with the ones measured. This demonstrates the accuracy of the identified parameters and the validity of the proposed heat transfer simulation technique.

2) The heat flux of Aqua gas flame around the preheating gas spouts is 50% larger than that of LPG flame while the total calorific value of Aqua gas is 25% smaller than that of LPG. This result shows that it is not appropriate to evaluate the thermal effect of preheating only from the total calorific value.

3) The calculated time until the plate face temperature to exceed the steel's kindling temperature almost agrees with the minimum piercing time observed in the piercing tests of Aqua gas and LPG. It becomes possible to anticipate the piercing time by numerical simulation for the first time.

Key Words: Heat transfer, Oxy-fuel cutting, Aqua gas, Inverse heat, Inverse heat conduction problem,

****

Prof. Naoki OSAWA
Department of Naval Architecture and Ocean Engineering
Osaka University
2-1 Yamadaoka, Suita, Osaka 565-0871
TEL +81-6-6879-7576 FAX +81-6-6879-7594
E-mail: osawa@naoe.eng.osaka-u.ac.jp

1. INTRODUCTION

Thermal cutting is widely used in the manufacturing of heavy equipment and construction of structural members for steel structures. In recent years, the demand for heavy thick steel plates with over 50mm thickness is growing up as upsizing of ships, offshore structures and buildings. Oxy-fuel cutting is the only cutting mean for these thick plates. Oxy-fuel cutting has been gaining renewed attention.

The function of the preheating flame in Oxy-fuel cutting was studied by Suitsu and Yasuda (1960, 1961) and Nakanishi (1968a, 1968b, 1968c), but the relation between the preheating flame conditions (fuel gas, gas conditions, the total calorific value, etc.) and the cutting performances (cutting speed, kerf quality, thermal distortion, etc.) has not been fully clarified yet. On this account, the adjustment of preheating flame has not been carried out by the automatic operation, but by skilled workers. In these days, the shortage of skilled workers has become critical, and it is strongly desired to automate this process.

In recent years, there is a move afoot to use Oxy-hydrogen cutting in industries. The use of hydrogen can reduce the greenhouse gas emission. It is reported that the hydrogen preheating reduces the thermal distortion of work pieces and it provides the improvement in the cutting performance. The precise mechanism of these improvements has not been clarified yet, and it is difficult to optimize the hydrogen preheating flame. For this reason, Oxy-hydrogen cutting has not become widespread.

It is expected that the preheating flame adjustment can be automated and it becomes easier to optimize the Oxy-hydrogen cutting condition if the relation between the preheating flame conditions and the cutting performance is clarified. This can be achieved by examining closely the relation between the flame conditions and the thermal effect. It is difficult to examine the thermal effect during Oxy-fuel cutting because both the heat transfer between the gas flame and the work piece and the exothermic reaction between the oxygen and the iron arise. The study of the thermal effects in piercing processes is a good way to get things started.

There are some studies on the thermal effect of preheating in piercing processes (e.g., Sato et al., 2008), but they failed to give a simple explanation on the relation between the heat input and the piercing performance. In most of these studies, the heat input was estimated from the total caloric value of the fuel gas, and the heat flux was not examined directly. It is considered that the direct heat flux estimation is needed to clarify the heat effect. Terasaki et al. (2009) examined the heat flux in Oxy-fuel cutting process quantitatively by using the heat flux determination technique proposed by Tsuji and Okumura (1977). In this flux determination technique, the heat flux distribution around the torch is assumed to remain unchanged with time. This approximation is not valid for spot heating cases in which the work piece temperature rises remarkably. Terasaki's results cannot be utilized in the study of piercing processes.

The authors (Osawa et al., 2008) developed a generic algorithms (GA)-based heat transfer estimation technique which can be applied to the cases where the heating face temperature exceeds the steel's kindling temperature. The relation between the flame condition and the heat transfer can be examined with a high degree of precision by using this technique. In their study, the generic representation of heat transfer parameters was developed for line heating analyses. It is needed to modify the generic representation so that it can represent the features of the preheating flame in Oxy-fuel cutting.

In this study, the author's GA-based heat transfer estimation technique is modified so that it can be applied to the analyses of preheating processes. The validity of the proposed technique and the accuracy of the identified parameters are examined by comparing the measured and calculated plate temperatures during spot heating tests. Aqua gas (combining propane gas with hydrogen and oxygen generated through water electrolysis) and LPG are used as preheating gas. The plate temperature during piercing process is calculated using these identified parameters, and the piercing performance is estimated by calculating the time until the plate face temperature reaches the kindling temperature. The validity of the proposed piercing performance estimation method is examined by comparing the estimated and measured minimum piercing times.

2. THEORY

2.1. Parameters for Heat Transfer between Gas Flame and Steel Plate

The authors (Tomita et al., 2001) measured the transient gas temperature field within the combustion flame during spot heating tests by laser induced fluorescence (LIF) measurement system. They found that the thermal-flow field of the heating gas becomes stable in an extremely short time and remains unchanged during spot heating. This means that the temperature of the gas adjacent to the plate T_G and local heat transfer coefficient α can be considered to remain nearly unchanged with time. This leads to a linear relationship between flux q and heating face temperature T_S.

Time histories of plate back surface temperature T_B are measured during a spot heating test. Time histories of flux and heating face temperature, q and T_S can be estimated by inverse heat conduction (IHC) analysis from the measured T_B. T_G and α can be identified by a linear regression analysis on the relation between q and T_S.

The authors (Osawa et al., 2004a, 2004b, 2007) proposed an IHC technique for the estimation of q and T_S. However, they sometimes failed to estimate them because the IHC problem is extremely sensitive to measurement errors. This problem can be overcome by estimating time-independent T_G and α directly. The authors (Osawa et al., 2008) proposed a generic algorithms (GA)-based direct identification technique for T_G and α. The validity of this technique was demonstrated by comparing the identified T_G and the one measured by LIF system.

2.2. Generic Representation of Heat Transfer Parameters

Hereafter, r denotes the distance from the nozzle center, and r_0, r_E the distances from the nozzle center to the spouts of preheating gas and the outer end of the analysis region. The region with $0<r<r_0$ is called 'inner region', and that with $r_0<r<r_E$ 'outer region'. In the GA analysis of Osawa et al. (2008), the generic representations was formulated so that T_G and α show their maximums at r=0. These representations cannot be used for Oxy-fuel cutting nozzles because T_G and α must show their maximum at $r=r_0$. We can assume the followings in the analyses of preheating for Oxy-fuel cutting: i) T_G shows its maximum at $r=r_0$ and the maximum T_G is close to the theoretical flame temperature. T_G approaches to the room temperature at $r=\infty$; ii) α shows its maximum at $r=r_0$. α approaches to the natural convection heat transfer coefficient when $r=\infty$. Based on these assumptions, T_G and α are represented as follows in this study:

(a) Set the upper and lower bound of T_G and α at r=0, r_0 and r_E:
$T_{C\min}, T_{C\max}, T_{0\min}, T_{0\max}, T_{E\min}, T_{E\max}, \alpha_{C\min}, \alpha_{C\max}, \alpha_{0\min}, \alpha_{0\max}, \alpha_{E\min}, \alpha_{E\max}$

(b) Give T_G and α at r=0, $r=r_0$ and $r=r_E$ as:

$$\left.\begin{aligned}
T_C &= T_{C,\min} + d_C\left(T_{C,\max} - T_{C,\min}\right)\\
\alpha_C &= \alpha_{C,\min} + e_C\left(\alpha_{C,\max} - \alpha_{C,\min}\right)\\
T_0 &= T_{0,\min} + d_0\left(T_{0,\max} - T_{0,\min}\right)\\
\alpha_0 &= \alpha_{0,\min} + e_0\left(\alpha_{0,\max} - \alpha_{0,\min}\right)\\
T_E &= T_{E,\min} + d_E\left(T_{E,\max} - T_{E,\min}\right)\\
\alpha_E &= \alpha_{E,\min} + e_E\left(\alpha_{E,\max} - \alpha_{E,\min}\right)
\end{aligned}\right\} \tag{1}$$

where, $d_C, d_0, d_E, e_C, e_0, e_E$ are real numbers ranging from 0 to 1.

(c) Arrange n_I number of control points (CP) in 'inner region', and enumerate them as $i_I=1,2,\ldots,n_I$ in order of increasing the distance from the spout ($r=r_0$). Give T_G and α at each CP as:

$$\left.\begin{aligned}
&T_{I1} = T_C + f_1\left(T_{\max} - T_C\right),\ \ \alpha_{I1} = \alpha_C + g_1\left(\alpha_{\max} - \alpha_C\right)\\
&T_{I2} = T_C + f_2\left(T_{I1} - T_C\right),\ \ \alpha_{I2} = \alpha_C + g_2\left(\alpha_{I1} - \alpha_C\right)\\
&\qquad\qquad\vdots
\end{aligned}\right\} \tag{2}$$

where, $f_1, g_1, f_2, g_2, \ldots$ are real numbers ranging from 0 to 1.

(d) In the same manner as (c), Arrange n_O number of CPs in 'outer region', and enumerate them as $i_O=1,2,\ldots,n_O$ in order of increasing the distance from the spout ($r=r_0$). Give T_G and α at each CP as:

$$\left.\begin{array}{l} T_{O1} = T_E + h_{O1}\left(T_{\max} - T_E\right),\ \ \alpha_{O1} = \alpha_E + k_{O1}\left(\alpha_{\max} - \alpha_E\right) \\ T_{O2} = T_E + h_{O2}\left(T_{O1} - T_E\right),\ \ \alpha_{O2} = \alpha_E + k_{O2}\left(\alpha_{O1} - \alpha_E\right) \\ \qquad\qquad \vdots \end{array}\right\} \tag{3}$$

where, $h_1, k_1, h_2, k_2, \ldots$ are real numbers ranging from 0 to 1.

(e) T_G and α between CPs are given by linear or 3rd order spline interpolation. $2\times 3 + 2\times n_I + 2\times n_O$ number of real numbers $d_C, d_0, d_E, e_C, e_0, e_E$, $f_1, g_1, f_2, g_2, \ldots$, $h_1, k_1, h_2, k_2, \ldots$ are the genes of GA analysis. An example of generic representation of T_G and α is shown in Fig. 1.

2.3. Fitness Function

The distributions of T_G and α are identified by carrying out spot heating tests of thin circular steel plates. Let $B_{J,K}$ be the measured plate back face temperature at the J-th measurement point ($J = 1,2,\ldots,N_B$) at time t_K ($K = 1,2,\ldots,N_T$), and $Y_{J,K}$ be the calculated temperature at the same point and same time. The fitness function E is defined as:

$$E = \frac{\sum_{K=1}^{N_T}\sum_{J=1}^{N_B}\left(Y_{J,K} - B_{J,K}\right)^2}{\sum_{K=1}^{N_T}\sum_{J=1}^{N_B}\left(B_{J,K}\right)^2} \tag{4}$$

E in Eq. (4) approaches to zero when the calculated back face temperatures agree well with the measured ones. The genes $d_C, d_0, d_E, e_C, e_0, e_E$, $f_1, g_1, f_2, g_2, \ldots$, $h_1, k_1, h_2, k_2, \ldots$ are optimized by GA analysis so that E is minimized.

3. IDENTIFICATION OF THE HEAT TRANSFER PARAMETERS

3.1. Spot Heating Tests

A circular mild steel disk of diameter d=300mm and 6mm thickness, shown in Fig. 2, is arranged horizontally and a preheating nozzle is positioned above the disk. The back surface of the disk is coated with a heat insulating material, and the center of the plate is heated by Aqua gas (52%H_2-22%C_3H_8-26%O_2) and LPG flame. Koike Sanso Kogyo type 6023 gas cutting torch was used, and Koike Sanso Kogyo types 105A-2 (for Aqua gas) and 106-2 (for LPG) were used for gas nozzles. These nozzles are suitable for cutting of steel plates with the thickness ranging from 15mm to 30mm. The spout geometries of the nozzles are shown in Fig. 3. The distances from the nozzle center to the preheating gas spouts, r0, is 3.0mm for both nozzles. The thickness of the test specimen (6mm) is much smaller than the recommended thickness (>15mm) because it is needed to increase the responsiveness of the back face temperature to the heat flux enough to suppress the ill-posedness of the IHC problem.

The pressure and the flow of the fuel gas and oxygen are shown in Table 1. The gas conditions for LPG are chosen by following the manufacturers recommendation for piercing process. Those for Aqua Gas are optimized by the authors in trial and error manner. The white corn length of gas flame was about 5mm for both gases. The distance between the work piece and the nozzle was 6mm. The pressure and flow were controlled by mass-flow rate sensors Yamatake CMS500 (for Aqua gas), CMQ200 (for LPG), CMS50 (for preheating oxygen) and CMS500 (for cutting oxygen). The total caloric values of each gas are also presented in Table 1. These values are calculated by assuming that the caloric value of LPG and C_3H_8 are 92.6MJ/m^3. Table 1 shows that the total caloric value of Aqua gas is about 75% of that of LPG.

The time histories of the plate back face temperature were measured by K-type thermoelectric couples (TCs) with a sheath diameter of 0.1mm welded on the plate back surface. The outputs of thermocouples were recorded on a personal computer every 0.5 sec. As shown in Fig. 4, TCs were arranged in a radial direction from the center to a point 104mm away from the center. The intervals of the points are 2mm for $r \leq 12$mm, 4mm for $12\text{mm} < r \leq 40$mm and 8mm for $r > 40$mm. For $r > 0$, the average of two measurements for the same r is taken as the representative value. In the tests, heating ceased within about 5 seconds. The gas torch was controlled by a welding robot FANUC ARC Mate DR-4000.

3.2. Optimization Analysis

$Y_{J,K}$ in Eq. (4) are calculated by carrying out axisymmetric finite element (FE) direct heat conduction (DHC) analyses in which $T_G(r)$ and $\alpha(r)$ represented by Eqs. (1), (2) and (3) are applied as boundary conditions.

The temperature dependencies of the material properties shown in Fig. 5 are used. DHC analysis is performed by using an in-house axisymmetric thermal FE code. The FE mesh and its dimensions are shown in Fig. 6 and Table 2. The FE model comprises 4 node isoparametric quadrilateral elements, and the back surface is assumed to be adiabatic. The initial temperature is 300K. The convective heat transfer between plate and air is evaluated at the outer end, and its coefficient is 480 W/(m^{2}K). In time integration, iterative calculation by Newman's method is repeated till the residual temperature norm becomes less than 10^{-6} times as much as the nodal temperature norm. The numerical damping is 0.01, and the time increment ranges from 10^{-4} to 5×10^{-2} sec.

The GA analyses are carried out by using the commercial optimization software, Optimus 5.2 (Noesis Solutions, 2006). The genes $d_C, d_0, d_E, e_C, e_0, e_E$, $f_1, g_1, f_2, g_2, \ldots$, $h_1, k_1, h_2, k_2, \ldots$ are optimized so that E in Eq. (4) is minimized by Self-Adaptive-Evolution algorithm (Schwefel, 1981).

Table 3 shows the upper and lower bound of T_G and α at r=0, r_0 and r_E. CPs are arranged at r=1.2, 1.6, 1.8 mm for ‘inner region’, and at r=4.28, 7.32, 13.4, 21.0, 32.4 mm for ‘outer region’. T_G and α between CPs are estimated by linear interpolation because the difference in the calculated back face temperatures derived from spline interpolation and that from linear interpolation is negligible. The control parameters of self-adaptive evolution are shown in Table 4.

3.3. The Heat Transfer Parameters: Results

The identified T_G and α for Aqua gas and LPG are shown in Fig. 7 and Fig. 8. $Y_{J,K}$ in Eq. (4) can be calculated by DHC analysis using these parameters as the thermal boundary conditions. The accuracy of the identified parameters can be examined by comparing $Y_{J,K}$ with $B_{J,K}$. The DHC analysis is performed by the FE code used in the GA analyses. The material properties shown in Fig. 5 and FE mesh shown in Fig. 6 are employed, and the calculation conditions are the same as those for IHC analysis. Fig. 9 and Fig. 10 compare the measured and calculated back surface temperatures, which coincide well. These results demonstrate the accuracy of the identified parameters, and the validity of the hypotheses on heat transfer between flame and plate.

3.4. The Heat Flux during Spot Heating

Fig. 11 and Fig. 12 show the calculated heat flux distribution q(t;r) at time t=0.5, 2.5 and 4.5 sec. for Aqua gas and LPG. These figures show that q decreases with time. q is the highest at r=r0 for Aqua gas while at the center (r=0) for LPG, and q within $r_0 < r < 12$mm of Aqua gas is about 50% larger than that of LPG. This means that the heat transfer of Aqua gas is larger than that of LPG even though the total caloric value of Aqua gas is smaller than LPG as shown in Table 1.

Fig. 13 shows the change of the ratios of T_G and α of Aqua gas to those of LPG with respect to r. This figure shows that these ratios show their maximum (about 145% for T_G and α) at r=4.5mm, and the ratio of α is maintained at this high level within $r \leq 12$mm while the ratio of T_G decreases with r rapidly. It is considered that the superiority of Aqua gas in α is the main cause of the negative correlation between the total caloric value and the heat flux. The burning velocity of hydrogen is about 3.4 times larger than LPG. This makes that the flow rate of Aqua gas is about 2.5 times larger than that of LPG. It is assumed that this difference makes the impinging jet heat transfer of Aqua gas becomes larger than that of LPG. The results described above show that it is not appropriate to evaluate the thermal effect of preheating only from the total calorific value.

4. ESTIMATION OF PIERCING PERFORMANCES

4.1. Piercing Tests

Rectangular steel plates with length 200mm, width 200mm and thickness 12mm shown in Fig. 14 were heated by Aqua gas and LPG preheating gas flame. The cutting torch was located at the point 50mm apart from two sides of the plate. The piercing conditions (nozzle, the gas conditions and nozzle height) are the same as those shown in Table 1. The thickness (12mm) is comparable with the recommended thickness of the cutting nozzles (15mm to 30mm).

The nozzle height was kept at 6mm during preheating. When the preheating finished, the torch was moved 10mm upward and the cutting oxygen was started to supply. The flow rate and pressure of the cutting oxygen was 150 *l*/min and 0.3MPa. The 'minimum piercing time' was measured by gradually extending the preheating time 5 sec. at a trial until the plate was successfully pierced. The temperature distribution on the plate heating face was measured by an infrared camera FLIR SYSTEM SC620NTSC. The radiation factor 0.97 was used in the temperature measurements.

The measured the 'minimum piercing time' was 15sec. for Aqua gas and 50sec. for LPG. It was observed that the diameter of the area in which the temperature exceeded the steel's kindling temperature (about 1200K) at the end of the preheating was larger than 10mm for the cases where the plate was successfully pierced.

4.2. Plate Temperature Estimation during Piercing Tests

The authors (Osawa et al., 2004b) showed that the plate temperature can be estimated accurately by assuming the T_G and α remains unchanged even if the heating face temperature exceeds 1000K. This leads us to an assumption that it is possible to estimate the time until the plate face temperature to exceed the steel's kindling temperature in the piercing tests by using T_G and α identified in the spot heating tests.

The plate temperature during the preheating process is calculated by using the FE code used in the GA analyses. The material properties shown in Fig. 5 and FE mesh shown in Fig. 15 are employed. The material properties and the calculation conditions are the same as those for IHC analysis. This FE model is an axysymmetric model of a circular plate with radius of 60mm, and it comprises 4 node isoparametric quadrilateral elements. The element edge length ranges from 0.1mm to 6.95mm in radial direction and from 0.1mm to 2.02mm in through-thickness direction.

Fig. 16 shows the calculated plate heating face temperatures at r=0, 3mm and 6mm during piercing tests preheated by Aqua gas and LPG. Let $t_{6mm,\ 1200K}$ be the time until the heating face temperature at r=6mm to exceed the steel's kindling temperature (1200K). It is shown that $t_{6mm,\ 1200K}$ is 13.5sec. for Aqua gas and 43.0sec. for LPG.

The results of the infrared camera measurements lead us to an assumption that the prerequisite for the success of piercing is the generation of a plate surface area with the diameter larger than 10mm within which the heating face temperature exceeds 1200K. Therefore, it can be considered that $t_{6mm,\ 1200K}$ approximately equal to the minimum piercing time. The calculated values of $t_{6mm,\ 1200K}$ (Aqua gas: 13.5sec, LPG:43.0sec.) almost agree with the measured minimum piercing times (Aqua gas: 15sec, LPG: 50sec.).

Fig. 17 (a) and (b) show the temperature distributions on the cross-section of the plate at the end of the preheating (Aqua gas: 15sec., LPG: 50sec.). These figures are illustrated upside down, and the lower surface is the heating face. The temperature distributions on the heating face of Aqua gas and LPG are generally similar while the cross-sectional temperature distributions are quite different. The region in which the temperature exceeds the mechanical melting point (1000K) reaches the back face for LPG while its border is at the midpoint of the cross section. This shows that the volume of inherent strain generation region (that is, the degree of the thermal distortion) is not positively correlated with the magnitude of the heat flux.

From the results described above, we can conclude that the plate temperature during piercing preheating process can be calculated with a high degree of accuracy by using T_G and α identified in the spot heating tests. It becomes possible to anticipate the piercing time by numerical simulation for the first time.

5. CONCLUSIONS

A generic algorithms (GA)-based identification technique for the heat transfer parameters, the gas temperature adjacent to the plate, T_G, and the local heat transfer coefficient, α, of the preheating gas flame of Oxy-fuel cutting is proposed. The validity of the proposed technique and the accuracy of the identified parameters are examined by comparing the measured and calculated plate back face temperatures during spot heating tests. Aqua gas and LPG are used as preheating gas in these tests. The minimum piercing time is estimated by calculating the time until the plate heating face temperature reaches the kindling temperature. The validity of the proposed piercing performance estimation method is examined by comparing the estimated and measured minimum piercing times for Aqua gas and LPG. As results, the followings are found.

1) The plate temperatures during spot heating tests calculated by using the identified T_G and α agree well with the ones measured. This demonstrates the accuracy of the identified parameters and the validity of the proposed heat transfer simulation technique.

2) The heat flux of Aqua gas flame around the preheating gas spouts is 50% larger than that of LPG flame while the total calorific value of Aqua gas is 25% smaller than that of LPG. This result shows that it is not appropriate to evaluate the thermal effect of preheating only from the total calorific value.

3) The calculated time until the plate face temperature to exceed the steel’s kindling temperature almost agrees with the minimum piercing time observed in the piercing tests of Aqua gas and LPG. It becomes possible to anticipate the piercing time by numerical simulation for the first time.

REFERENCES

Nakanishi, M (1968a) “Study of Preheating Flame on Oxygen Cutting (Report 1) −Examination of the Heating Effect on the Cut Material-”, Journal of the Japan Welding Society, 37, 8, pp. 839-844, 1968 (in Japanese).

Nakanishi, M (1968b) “Study of Preheating Flame on Oxygen Cutting (Report 2) −Activation Effect on the Material Surface-”, Journal of the Japan Welding Society, 37, 10, pp. 1108-1114, 1968 (in Japanese).

Nakanishi, M (1968c) “Study of Preheating Flame on Oxygen Cutting (Report 3) −Effect of Preheating Flame on Material Thickness to be Cut-”, Journal of the Japan Welding Society, 37, 11, pp. 1260-1287, 1968 (in Japanese).

Noesis Solutions (2006) “OPTIMUS 5.2 – Users Manual”.

Osawa N., Tomita Y., Hashimoto K., Matsuoka K. and Kikuchi K. (2004a) "Development of Heat Input Estimation Technique for Line-Heating Process based on Inverse Heat Conduction Analysis" Proc. ISOPE2004, IV, pp. 133-140.

Osawa, N, Tomita, Y, Hashimoto, K, Kikuchi, J (2004b) "Improvement of the Accuracy of Heat Input Estimation during Line Heating Process by using Regularization Method", Proc. the 9th Symposium on Practical Design of Ships and Offshore Floating Structures, pp. 974-981.

Osawa N., Hashimoto K., Sawamura J., Kikuchi J., Deguchi Y. and Yamaura T. (2007) "Development of Heat Input Estimation for Simulation of Shell Forming by Line-Heating", Computer Modeling in

Engineering & Sciences, 20, 1, pp. 43-53.

Osawa, N, Hashimoto, K, Sawamura, J, Tanaka, H (2008) “GA-based Heat Input Estimation Technique for Simulation of Shell Forming by Line-Heating”, Proc. 18th International Offshore and Polar Engineering Conference, pp. 285-290.

Sato, T, Yamamoto, Y., Kato, T, Takeda, T., Nagahori, M, Kamikihara, H (2008) “Influence of gas contents on characteristics of hydrogen-propane flame in oxyfuel gas cutting”, Preprints of the National Meeting of JWS, 83, pp. 78-79 (in Japanese).

Schwefel, H.P. (1981) “Numerical Optimization of Computer Models”, John Wiley & Sons, Chicester, New York.

Suitsu, K, Yasuda, T (1960) “Some Investigations Regarding Oxygen Cutting (Report 2) –Effect of Steel Temperature on the Cutting Efficiency-”, Journal of the Japan Welding Society, 29, 6, pp. 490-497 (in Japanese).

Suitsu, K, Yasuda, T (1961) “Some Investigations Regarding Oxygen Cutting (Report 5) –Effect of Preheat Variation on the Cutting Efficiency-”, Journal of the Japan Welding Society, 30, 10, pp. 733-739, 1961 (in Japanese).

Terasaki, T, Kitamura, T, Miyamoto, M (2009) “Heat input generated in plate by gas cutting process”, Journal of the Japan Society of Naval Architects and Ocean Engineers, 10, pp. 197-204 (in Japanese).

Tomita, Y, Osawa, N, Hashimoto, K, Shinkai, N, Sawamura, J, Matsuoka, K (2001): Study on Heat Transfer between Gas Flame and Plate during Line-Heating Process. In: Y.S. Wu, W.C. Cui and G.J. Zhou (ed) Practical Design of Ships and Other Floating Structures, Elsevier, pp. 389-396.

Tsuji, I, Okumura, Y (1977) "A Study on Line Heating Process for Plate Bending of Ship Steels," Trans. The West-Japan Soc. Naval Architects 76, pp.149-160 (in Japanese).

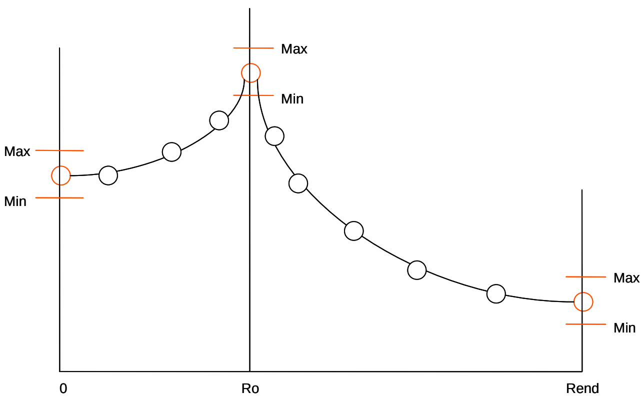

Fig. 1: Generic representation of the distribution of heat transient parameters.

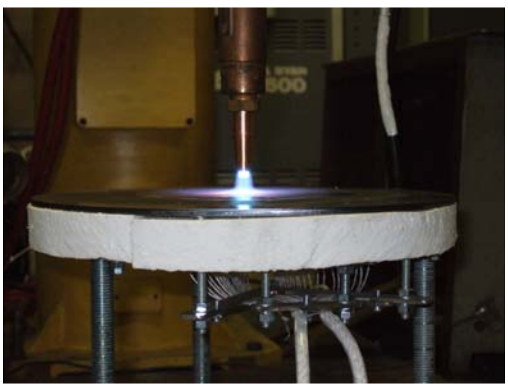

Fig. 2: Test specimen used in spot heating tests.

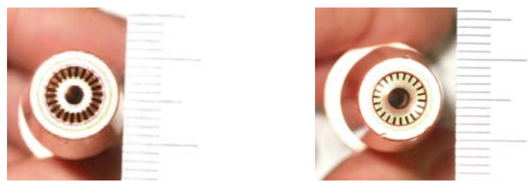

(a) Aqua gas (b) LPG

Fig. 3: Preheating gas nozzles for Aqua gas and LPG (#2 nozzle).

Table 1: Heating conditions employed in spot heating tests.

	Aqua gas	LPG
Distance btwn. nozzle and plate [mm]	6.0	6.0
Pressure of burning gas [MPa]	0.038	0.020
Flow of burning gas [*l*/min.]	16.0	6.0
Pressure of Oxigen [MPa]	0.053	0.072
Flow of Oxigen [*l*/min]	16.0	13.0
Togal calorific value [MJ/Hr.]	24.9	33.3

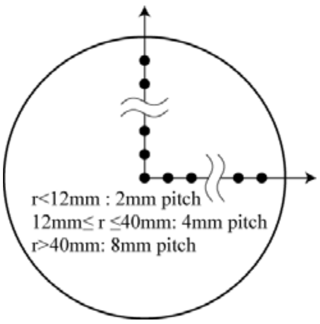

Fig. 4: Arrangement of thermocouples for spot heating tests.

Table 4: Control parameters of self-adaptive evolution employed in the analyses.

Random seed	1
Num. of parents	5
Sexuality	5
Population size	60
Initial step width	1
Average stopping stepwidth	0.01
Stepwidth mutation factor	1.3
Max. num. of iterations	30

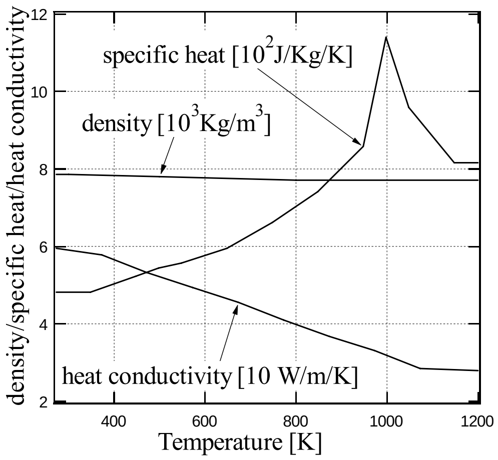

Fig. 5: Temperature dependency of the material properties.

Fig. 6: The FE mesh used in direct heat conduction analysis of spot heating tests.

Table 2: Model dimensions of the FE mesh for DHC analysis of the spot heating tests.

Model dimensions	0.3×0.006 (m)
Num. of Elements	$40 \times 40 \times 6$
Max./Min. element size in x dir	$3.44 / 13.8$ ($\times 10^{-3}$ m)
Max./Min. element size in y dir	$3.44 / 13.8$ ($\times 10^{-3}$ m)
Max./Min. element size in z dir	$5.04 / 16.8$ ($\times 10^{-4}$ m)

Table 3: The upper and lower bound of T_G and α at r=0, r_0 and r_E.

r	Heat transfer coefficient α [W/(m^{2}K)]		Gas temperature right on the plate T_G [K]	
	min.	max.	min.	max.
0	1900	2600	3400	3700
r_0	2500	3500	3800	4200
r_{end}	480	600	867	1500

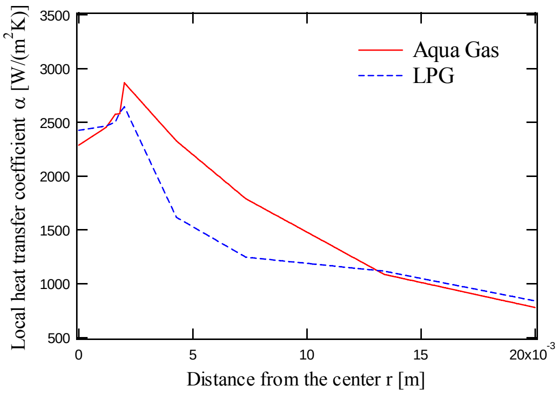

Fig. 7: Distributions of gas temperature right on the plate T_G during spot heating tests.

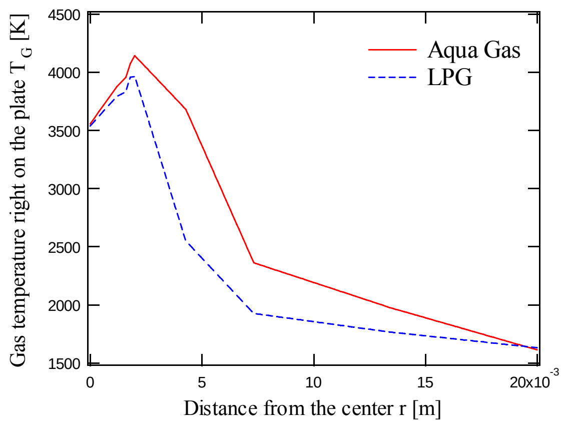

Fig. 8: Distributions of local heat transfer coefficient α during spot heating tests

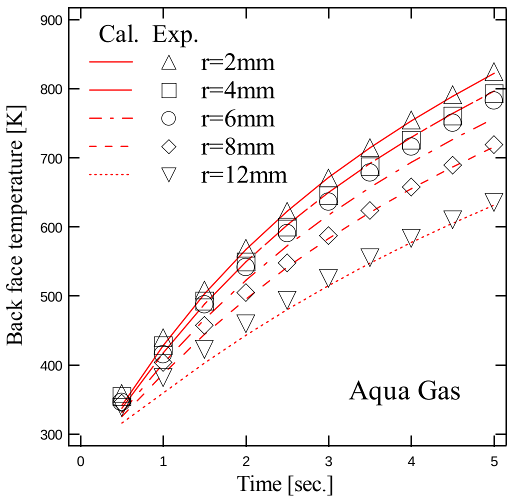

Fig. 9: Comparison of the measured plate back surface temperatures during spot heating test with the ones obtained by direct heat conduction analysis using the identified T_G and α of Aqua gas..

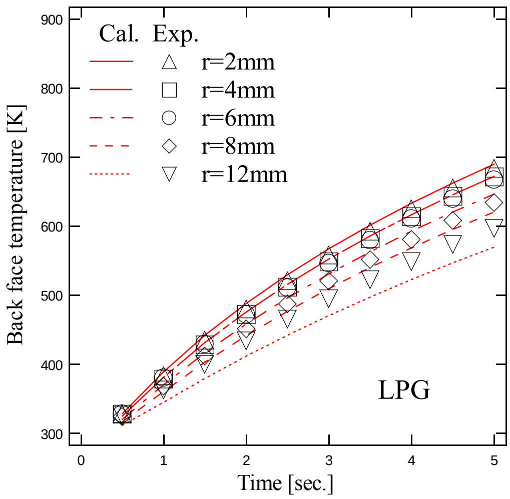

Fig. 10: Comparison of the measured plate back surface temperatures during spot heating test with the ones obtained by direct heat conduction analysis using the identified T_G and α of LPG.

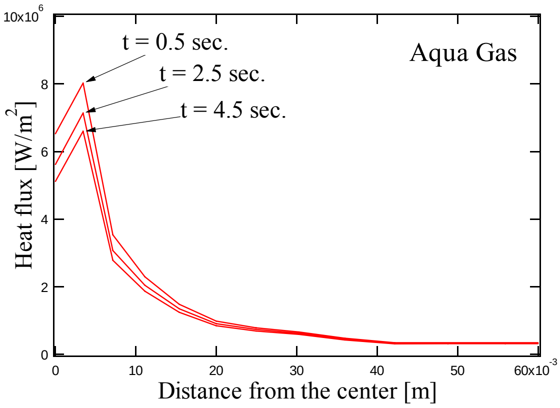

Fig. 11: Heat flux distribution during the spot heating test with aqua gas.

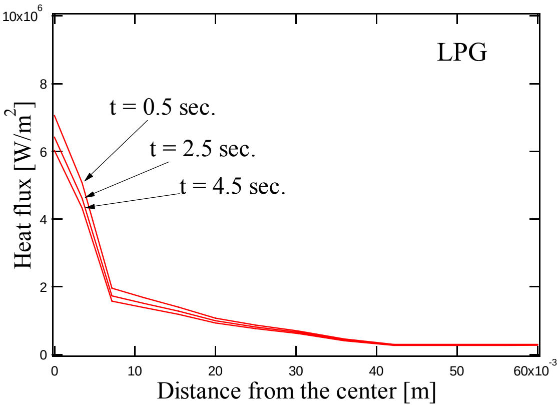

Fig. 12: Heat flux distribution during the spot heating test with LPG.

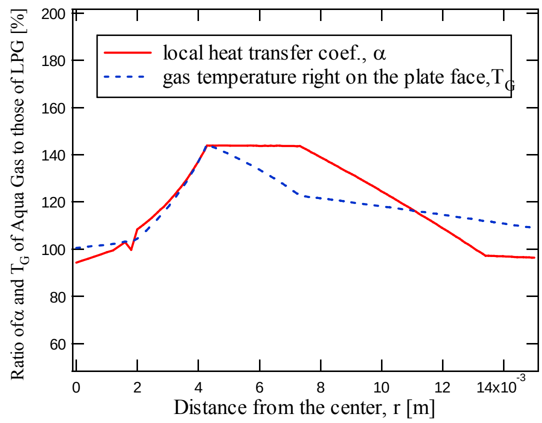

Fig. 13: Ratio of α and T_G of Aqua Gas to those of LPG.

Fig. 14: Test specimen used in piercing tests.

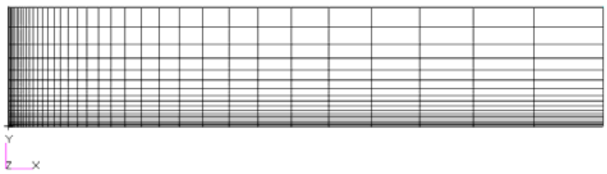

Fig. 15: The FE mesh used in direct heat conduction analysis of piercing tests.

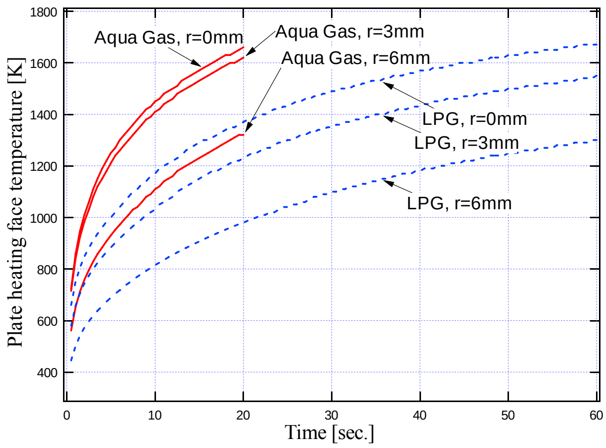

Fig. 16: Time histories of plate heating face during piercing tests.

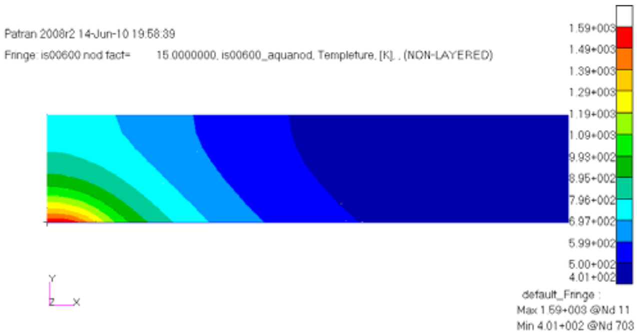

(a) Aqua Gas, time = 15sec.

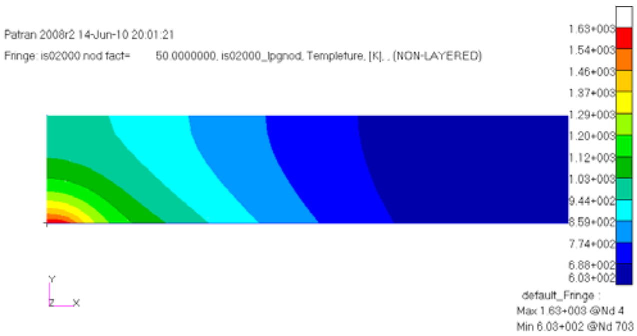

(b) LPG, time = 50sec.

Fig. 17: Plate temperature distributions at the times when the plate heating face temperature within a radius of 6mm from the torch center exceed the burning temperature of steel (about 1200K).